EURASIAN PHYSICAL TECHNICAL JOURNAL

2024, Volume 21, No. 2 (48)

https://doi.org/10.31489/2024No2/102-111

Received: 09/02/2024 Revised: 30/01/2024 Accepted: 17/06/2024 Published online: 29/06/2024

Research Article

UDC 537.87

INVESTIGATION OF CYCLIC PROPERTIES OF SOLAR AND GEOMAGNETIC ACTIVITIES: IMPLICATION FOR GLOBAL SURFACE TEMPERATURE VARIABILITY

Ibanga E.A.[1], Inyang E.P.[1], Agbo G.A.[2]

[1] Department of Physics, National Open University of Nigeria, Jabi, Abuja-Nigeria
[2] Department of Industrial Physics, Ebonyi State University, Abakaliki, Nigeria
*Corresponding author email: etidophysics@gmail.com

Abstract. *The cyclic properties of solar-geomagnetic activity and global surface temperature have been investigated using trend, frequency and time-frequency analyses. Results reveal that on decadal-to-centennial timescales, low-frequency cycles in the half-century (~49 to 56 years per cycle) and Gleisberg (~99 to 114 years per cycle) range run in the background of the Schwabe (~9 to 11 years per cycle) as the dominant cycle of solar-geomagnetic activity. The only dominant cycle in the global surface temperature series is the half-century cycle and suggests a possible causal link between it and solar-geomagnetic activity phenomena. Evolution of the amplitudes of the cycles is such that the Schwabe and Gleisberg periods have increased in power from the beginning of the series until the mid-20th century after which they declined. The half-century cycle decreased in amplitude after 1800 to the present. For geomagnetic activity, the amplitude of Gleisberg cycle increased from the beginning of the series around 2000 while the amplitudes of Schwabe and half-century cycles declined within the same interval, except the Schwabe cycle which amplitude increased rapidly after 1980 to the present. For the global surface temperature, the amplitudes of Gleisberg and half-century cycles have continuously increased from the beginning of the series while Schwabe cycle oscillates with very low amplitudes until 1980 after which it increased slightly. Evolution of the amplitudes of cycles of solar-gemagnetic activity suggests a recovery from Maunder Minimum and decline into a grand epsode most likely to be a minimum.*

Keywords: geomagnetic activity, solar activity, low-frequency cycle, grand episode, spectral power, global wavelet power.

1. Introduction

It is now known that the time series of solar and geomagnetic activities as well as climate phenomena are inherently characterized by multiple periodicities buried in noise, which may include the effects of interactions and nonlinearities. Detection and estimation of periodic components in forcing signals require the application of techniques that could eliminate or suppress the noisy background. Several techniques have been applied to study the periodic properties of the time series of solar activity, geomagnetic activity and climate change phenomena, using different proxies and on different temporal scales. Among such techniques include filtering to test for the existence of multiple periodicities and reveal trends of varying degrees and resolution of cyclicity of the forcing signals [1,2], frequency analysis based on spectral methods [3], deep learning and predictive models using neural network [4-6] and time-frequency analysis based on wavelet methods [7-9] and so on. Solar activity, characterized by variations in solar irradiance and sunspot numbers, follows an approximately 11-year cycle known as the solar cycle. Geomagnetic activity, influenced by solar wind and coronal mass ejections, is often quantified by indices such as the Ap and Kp indices. Both solar and

geomagnetic activities have been hypothesized to affect Earth's climate, but the extent and mechanisms of this influence remain subjects of ongoing research.

The arguments concerning climate change, and in particular the recent climate warming, are based on observations and predictions in terms of time and frequency of occurrences. For this purpose, wavelet analysis has been extensively explored. For solar and geomagnetic activities, once the dominant cycles have been revealed, their effects on and possible causal relationship to climate time series may become evident.

How and to what extent the evolution of temporal structures of solar-geomagnetic activity and climate interaction have contributed to the recently observed climate warming forms the basis of this study. The essence is to examine the cycles inherent in their temporal variability with a view to revealing the time-frequency patterns in the structures and how they may relate to and help to predict the near-future climate scenarios.

2. Data and Methods of Analysis

(i) Solar activity proxy comprised the annual mean sunspot number (R_Z) (1700-2020), obtained from World Data Centre (WDC), Sunspot Index and Long-term Solar Observations, http://www.sidc.be/silso/datafiles.

(ii) Geomagnetic activity proxy was characterised by antipodal activity (aa) index (1868-2020), obtained from NASA website at https://omniweb.gsfc.nasa.gov/form/dx1.html.

(iii) Global Surface Temperature Anomaly (dT) (HadCRUT5) and HadSST3 (1850-2023) obtained from Met Office Hadley Centre, https://www.metoffice.gov.uk/hadobs/hadcrut5/data/current/download.html

Time-series analyses comprising filtering, smoothing, trending, regression and curve fitting were performed on the relevant time series. The cyclic variabilities inherent in trends of the relevant phenomena were studied.

Spectral analysis derived from Fast Fourier Transforms (FFT) was performed to determine the strength of the cycles and establish the cyclic relationships among the phenomena under consideration.

To reveal the evolution of cycles in time and frequency of solar-geomagnetic activity and global surface temperature, time-frequency analysis using the continuous wavelet transforms was performed. The mother wavelet represents a family of functions [10] and is given as:

$$\psi(t)_{s,\tau} = \frac{1}{\sqrt{s}}\left(\frac{t-\tau}{s}\right) \quad (1)$$

where $s,\ \tau \epsilon R;\ s \neq 0$; s, τ are scaling (dilation or contraction) and translation (shifting) factors respectively while $\frac{1}{\sqrt{s}}$ is for the normalisation of energy across the different scales.

The computation of continuous wavelet coefficients is based on eqn. 2:

$$W_x(s,\tau) = \left|\frac{s}{\delta t}\right|^{-½} \sum_0^{N-1} \quad x(t)\psi^*\left(\left(\frac{t-\tau}{s}\right)\delta t\right) \quad (2)$$

where N is the time series length and $\left|\frac{s}{\delta t}\right|^{-½}$ is the normalization parameter of the wavelet function[10] and was obtained by dilating or contracting the wavelet scale, s and translating along localized time position, τ. Wavelet coefficients describe the contribution of the scale s to the time series x(t) at different time position τ.

In this study, the continuous wavelet transformation was performed using Morlet wavelet as the analyzing wavelet [11] and is expressed as:

$$\psi\left(\frac{t-\tau}{s}\right) = \pi^{-¼} e^{i\omega_0\left(\frac{t-\tau}{s}\right)} e^{-\left(\frac{t-\tau}{s}\right)^2/2} \quad (3)$$

where ω_0 is the wave number and is taken to be 6.0 in this case.

The wavelet spectral power $P(s,\tau)$ is computed as shown in eqn. 4.

$$P(s,\tau) = 2^s\left|W_{j,k}(t)\right|^2 \qquad j,k = 0,1,2,\ldots,N-1 \quad (4)$$

where, 2^s is the bias correction factor [12]. The scale s of the Morlet wavelet is related to Fourier frequency f as in eqn. 5:

$$\frac{1}{f} = \frac{4\pi s}{\omega_0 + \sqrt{2+\omega_0{}^2}} \quad (5)$$

The scale s is approximately equal to the reciprocal of the Fourier frequency, $s \approx \frac{1}{f}$ [13].

3. Results and Discussion

The eleven-year (Schwabe) annual mean cycles are numbered 1 in 1749 to 24 in 2014 Fig.1 (a). The grand episodes are clearly illustrated. The highest peak of the cycles occurred in the International Geophysical Year (1957) with $R = 269.5$. The observed minima $R_1 = 0$ in 1711, $R_2 = 0$ in 1810, $R_3 = 2.4$ and $R_4 = 4.2$ in 2008 give an average cycle length of 98.7 years (Gleissberg period).

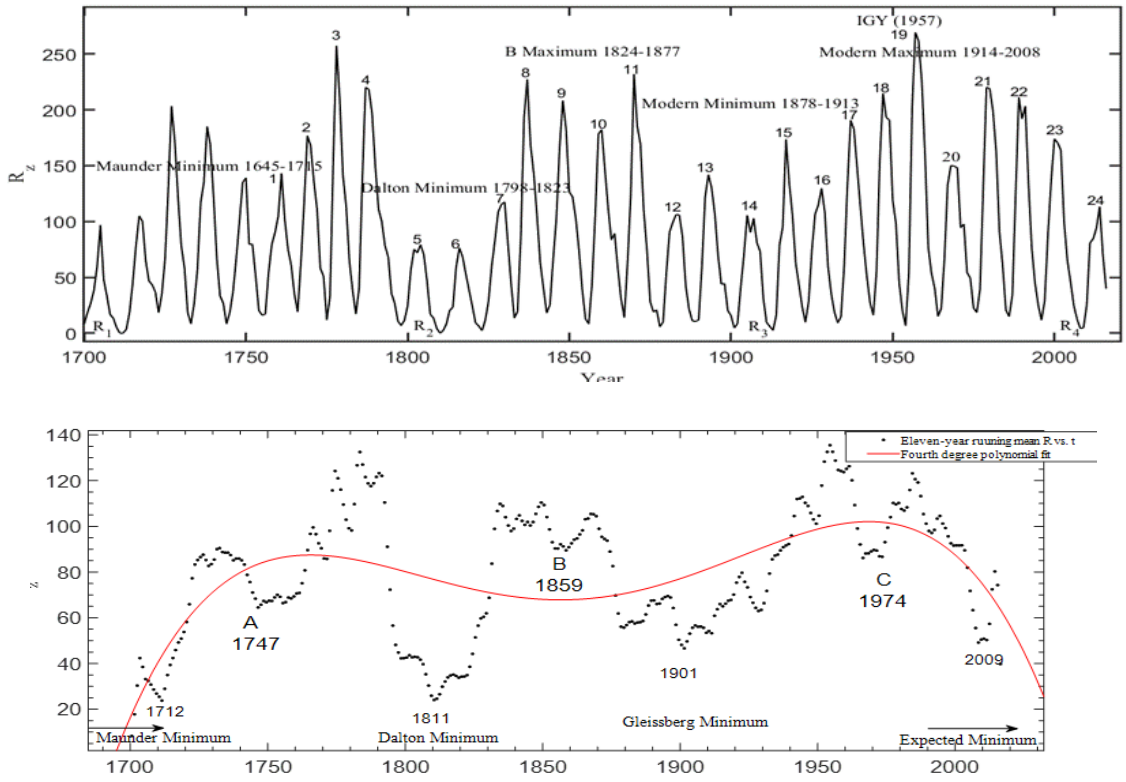

Fig.1. (a) Annual mean sunspot number (b) eleven-year running-mean with fourth-degree regression model

The eleven-year running-mean R_Z also reveals a minimum-to-minimum cycle of length ~99 years (Gleissberg period) Fig.1 (b). The maximum to maximum of the fourth-degree polynomial gives a low-frequency cycle of ~277 years but cycle length taken from the corresponding maxima of the eleven-year running mean is ~179 years. The average of the two values suggests a bi-centennial cycle (BC) of ~227 years. It is clear that subsequent minima after the Maunder Minimum were successively higher, which implies that solar activity has gradually been recovering (increasing in strength) after the grand minimum.

Quasi-grand episodes, laballed A, B, and C are approximately 114 years apart on the average (Gleissberg period range). Further still, the minimum-to-minimum, taking account of the quasi-minima, is approximately 52.4 years on the average. Therefore, sunspot activity of 11-, 52-, 114-year and 227-year periodicities have been identified using our trend analysis. For ease of reference, these cycles are herein labelled as Schwabe cycle (SB), half-century cycle (HC), Gleissberg cycle (GB) and bi-centennial cycle (BC) respectively. These cycles are in agreement with those found using other methods. For instance, Dergachev & Raspopov (2000), using sundry solar activity proxies such as total solar irradiance (TSI), carbon-14 (^{14}C) and Beryllium-ten (^{10}Be) levels and galactic cosmic ray (GCR), identified a 210-year SC.

The correlation of aa with R_Z is shown in Fig.2. The annual mean aa time series shows greater variability than the eleven-year running-mean (Fig. 2a) but are strongly correlated on the eleven-year solar activity cycle time scale (Fig. 2b). The correlation coefficient of the annual mean and eleven-year running mean aa and R_z time series are $r = 0.56$ and 0.87 respectively, within 95% confidence bounds. The relatively low value of r for the annual mean variability of aa is quantitative evidence of the prevalence of transient heliosphysical and interplanetary activities on shorter cycle-time scales, acting as background noise in concert with low frequency solar cycles. It is observed that annual mean aa variation is characterized by multiple peaks, comprising those that occur with peaks and those that occur in the declining phases of the

eleven-year sunspot activity cycles. The trend also reveals a dual peak B and C in SC19 and SC23. The peak A near the beginning of the time series corresponds to 1877 solar activity maximum. The quasi-minima marked a, b, c and d do not exhibit any consistent cycle lengths. The year marked d is not necessarily a minimum but is included to show the downward trend. It is also known that solar activity peaks of 1989 and 2003 were accompanied by severe space weather events. Although the filtering process tends to shift the position of the peaks of trended time series with respect to those of the annual mean variability, it is obvious from Fig. 2a that while the peak of solar activity occurred during the International Geophysical Year (IGY) 1957, the peak of geomagnetic activity occurred four solar cycles after, in 2003, evidently in the declining phase of solar activity low-frequency cycle.

Fig. 3 shows the annual mean global surface temperature represented by two recent time series HadSST3 (sea surface) and HadCRUT4 (land and sea) time series, together with their eleven-year running means and seventh-degree polynomial regression model of HadCRUT5, which closely fits both data and trend.

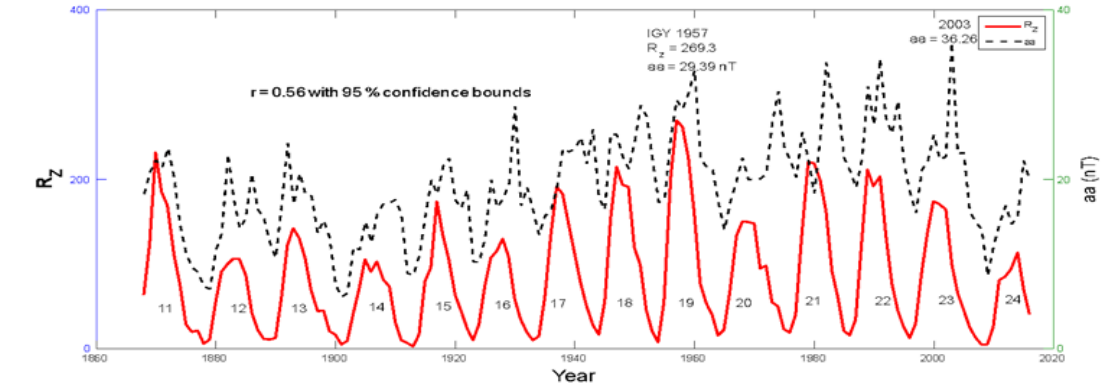

a)

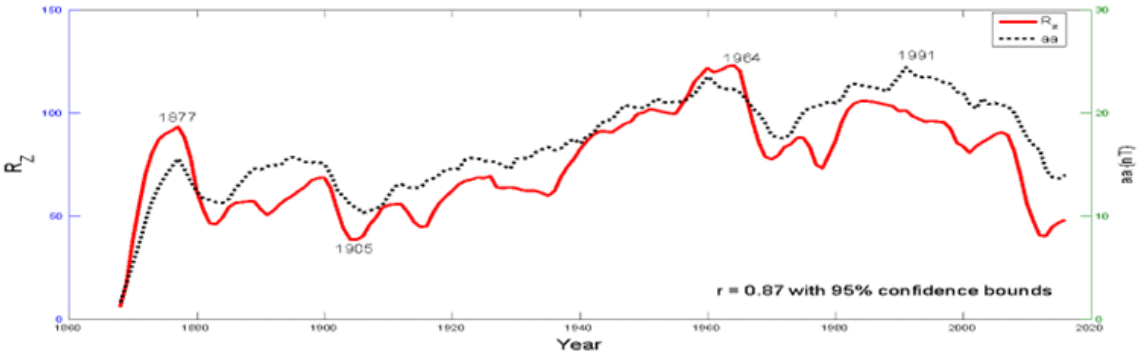

b)

Fig.2. Sunspot number versus geomagnetic activity (a) annual mean (b) eleven-year running mean

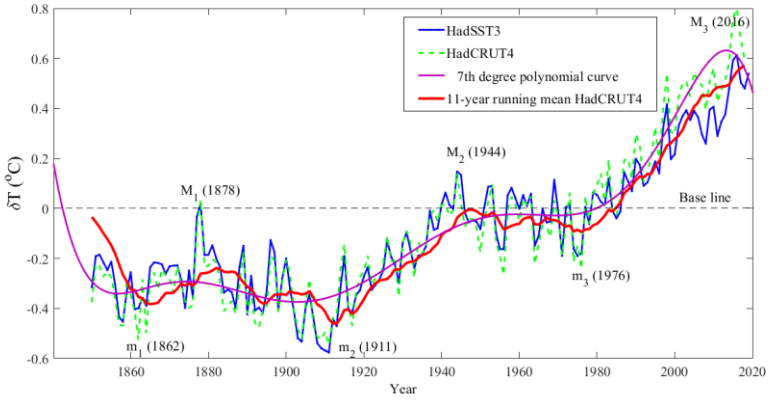

Fig.3: Global Sea surface temperature (HadCRUT5 & HadSST3) with the eleven- year running and the seventh-degree polynomial model

Clearly, the time series began in a descending phase, reached a minimum in 1911, and exhibited two maximum-to-maximum marked $M_1(1878)$ $M_2(1944)$ and $M_3(2016)$ of average cycle length of 64c. It also exhibits two minimum-to-minimum labelled $m_1(1862)$, $m_2(1911)$ and $m_3(1976)$ of average cycle length of 57 years. This suggests a global temperature cycle of an average period of 60 years (which is in the HC range). Identification of this cycle is crucial to the determination of the phenomenon that drives it. The spectral power of sun spot activity, antipodal geomagnetic activity and global surface temperature anomaly series are displayed (Fig. 4).

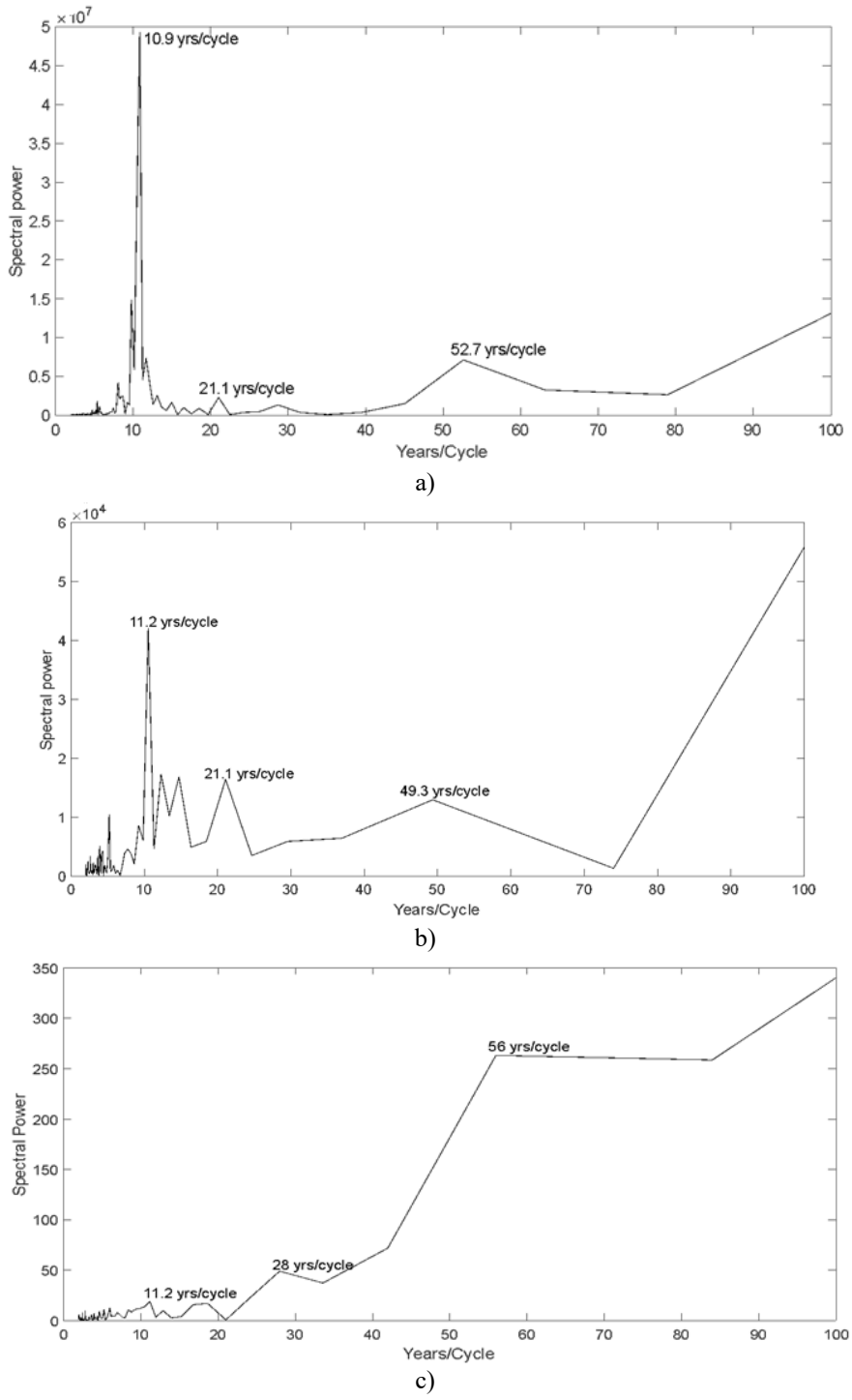

Fig.4. Periodogram of (a) solar activity and (b) geomagnetic activity proxies (c) global surface temperature anomaly

The most prominent cycle of solar and geomagnetic activities is the SBC followed in order of magnitude by the HC (Fig. 4a). The same is the case for geomagnetic activity (Fig. 4b), except that the HC is of slightly lower cycle length (49.3 years/cycle) compared to that of solar activity (52.7 years/cycle). The most prominent cycle of global surface temperature anomaly is the HC, ~56-years (Fig. 4c). Other less prominent cycles are also labelled. The apparent similarity of the spectral powers of solar and geomagnetic activities provides further evidence of the correlation that exists between the two series. Spectral analysis allows us to examine the frequency components of these activities, revealing patterns that might not be immediately obvious in the time domain. By observing that both solar and geomagnetic activities exhibit similar spectral power distributions, we can infer that they are influenced by common factors or mechanisms. This similarity suggests a strong connection, likely driven by the Sun's influence on the Earth's magnetic field. For example, solar phenomena such as sunspots, solar flares, and coronal mass ejections can significantly impact geomagnetic activity, causing variations in the Earth's magnetosphere. The alignment in their spectral powers indicates that changes in solar activity are mirrored by corresponding changes in geomagnetic activity, reinforcing the idea of a dynamic and interdependent relationship between these two series.

By comparison with the spectral powers of solar and geomagnetic activities, it is clear that the spectral power of global surface temperature anomaly (Fig. 4c) follows the same pattern of variability, with some degree of modulation. It implies that global surface temperature variability has components that are attributable to the variability of solar and geomagnetic activities. Fig. 5 (a) shows the continuous wavelet transform of sunspot activity. All the cycles increase in level between 1750 and 2000 except the HC which diminishes after 1850. SB and GB reached maximum levels between 1950 and 2000. The global wavelet power (Fig. 5b) exhibits three peaks corresponding to SB, HC and GB, with SB and GB as the most dominant cycles.

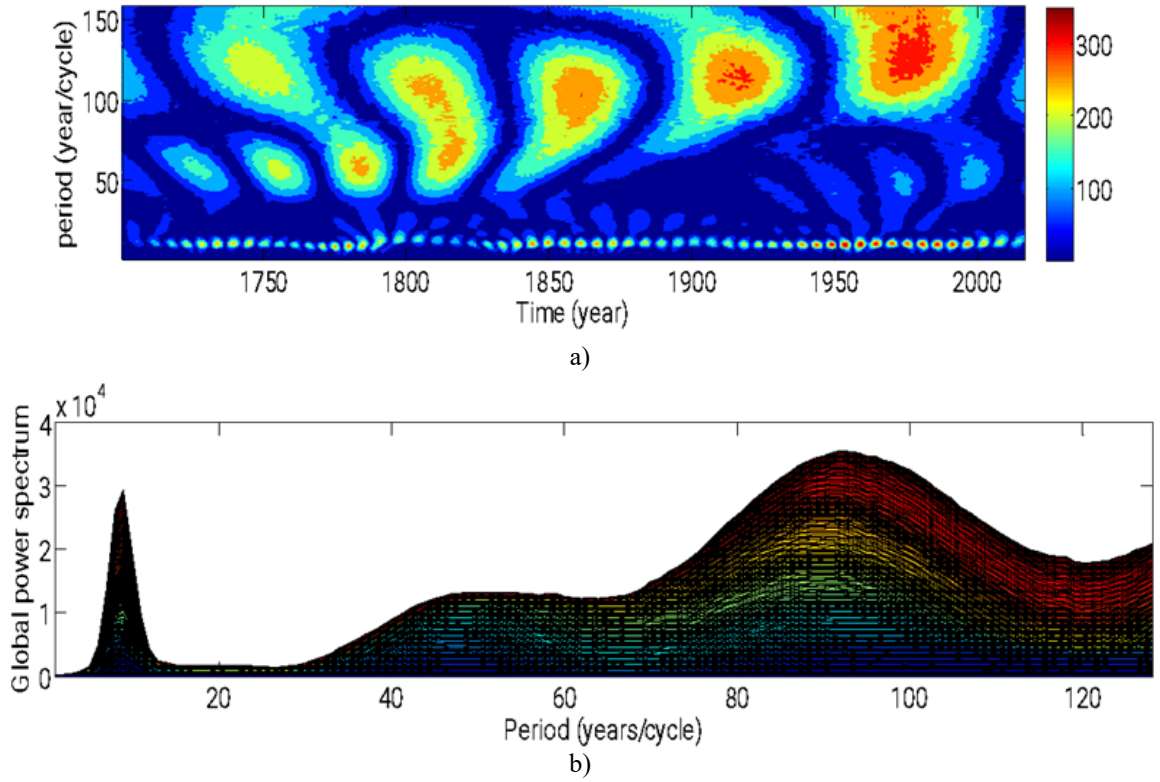

Fig.5. Continuous wavelet transforms and global wavelet power spectrum of sunspot activity.

Fig. 6 displays the plots of continuous wavelet transform and the global power spectrum of geomagnetic activity. GB is the most prominent cycle. It increases in level to a maximum between 1970 and early 2000s. HC also followed the same pattern of variability, although it is less prominent. The SB is less prominent compared to GB and HC. In addition to the three cycles, it is apparent that a lower frequency cycle, possibly of 150-year cycle is present and is localized between 1940 and 2000 (Fig. 6a). The global

power spectrum (Fig. 6b) reveals three peaks corresponding to the SB, HC and GB respectively, and possible existence a lower frequency cycle in the 150-year range. The strongest cycle is the GB followed by the HC.

The continuous wavelet transform and global wavelet power spectrum of the global surface temperature are shown in Fig. 7. Fig. 7a shows that HC increases in strength from the beginning the series to a maximum in. It is noticed that cycles with higher periods (above 150 years/cycle) are localized around 1900 and 2000.

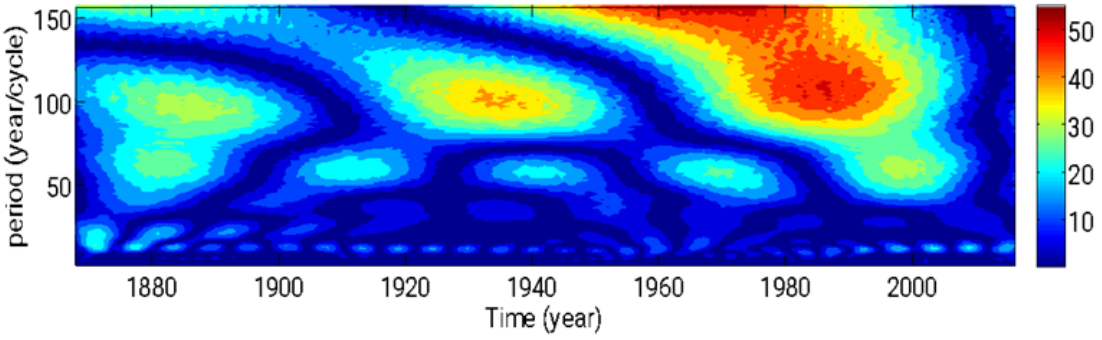

a)

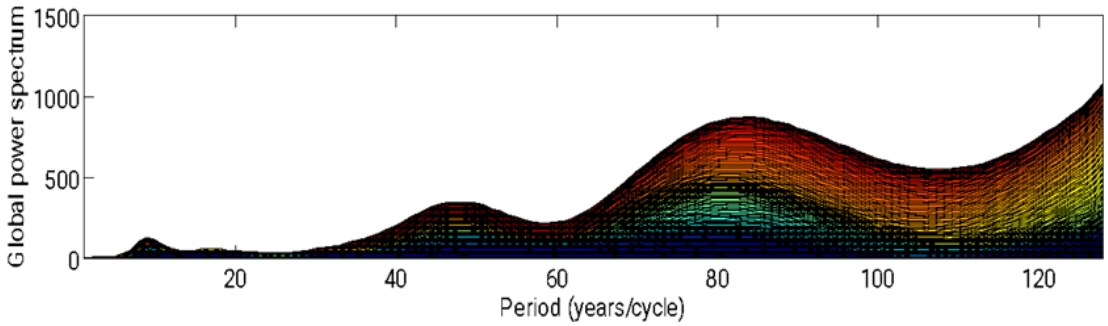

b)

Fig.6. (a) Continuous wavelet transforms coefficients (b) Global wavelet power spectrum of geomagnetic activity

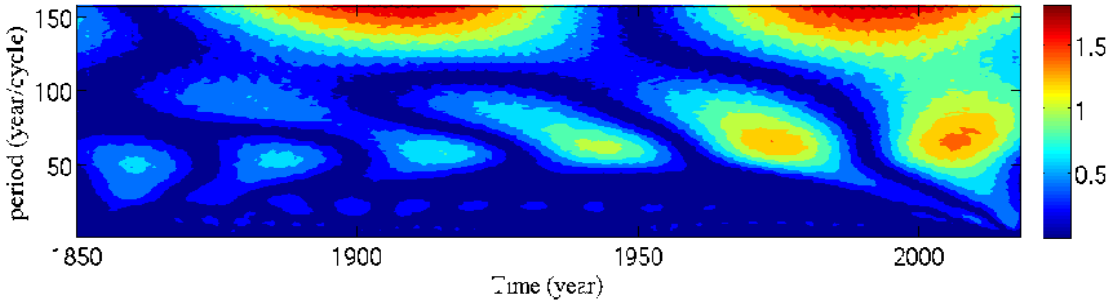

a)

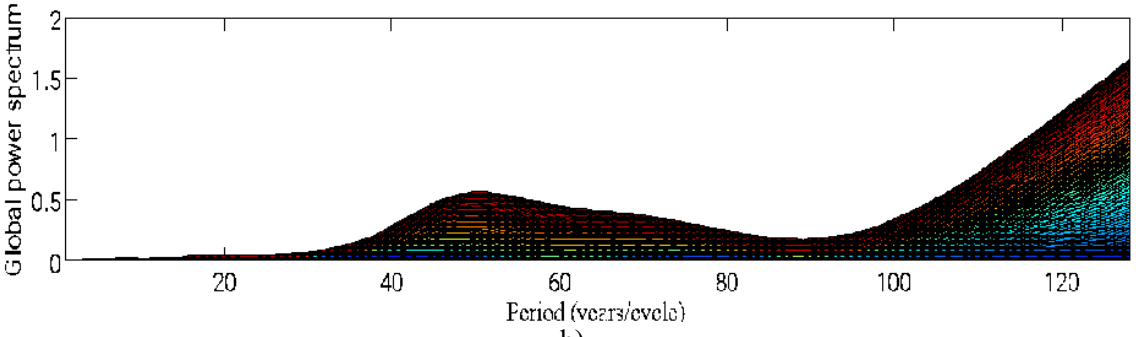

b)

Fig.7. Plots of continuous wavelet transform coefficients and global wavelet power spectrum of global surface temperature

Fig. 7b shows a prominent peak only at 51 years/cycle corresponding to the HC. There appears to be a low-frequency cycle, possibly in the 150 years range. The HC component of cyclicity clearly exists in all the three times series. It is apparent that global surface temperature, solar activity and geomagnetic activity have a possible causal link through the HC and, possibly, lower frequency cycles.

It is clear that the low frequency cycles have continued to increase in level in all the three series. It suggests that the low frequency components of solar and geomagnetic activities possibly contribute to the current climate warming scenario. Fig. 8 shows the trends in the evolution of the amplitudes of the SB, HC and GB of sunspot activity, geomagnetic activity and global surface temperature.

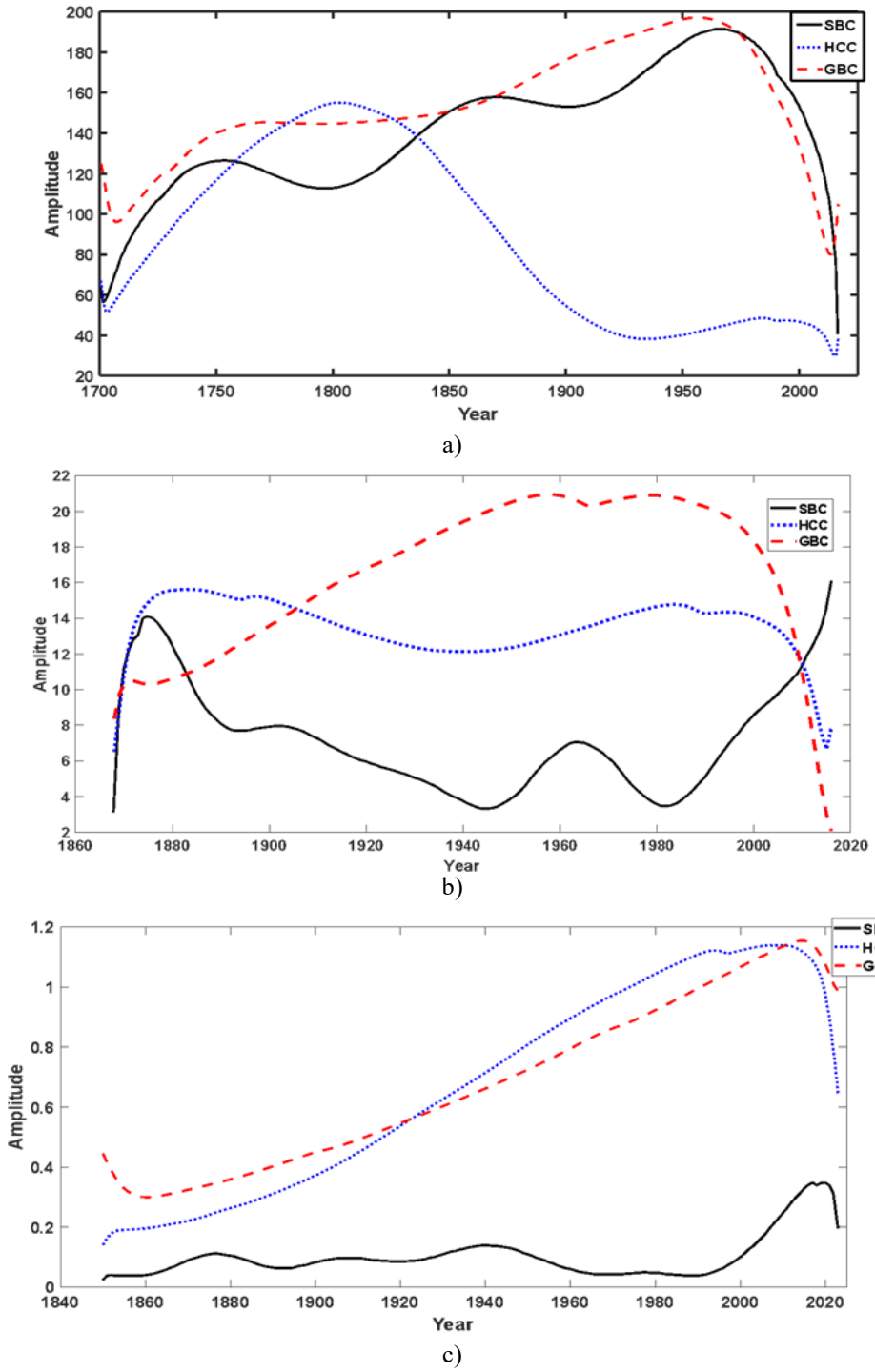

Fig.8. Evolution of the amplitudes (a) (Rz) (b) aa (c) dT

In Fig. 8a, it is found that between 1700 and 1780 the amplitude of GB was higher than those of SB and HC. The amplitude of HC was higher than both the SB and GB from 1781 and 1826, reaching its peak in 1802 and declining thence after. From 1836, the amplitude of HC was lower than those of SB and GB. The SB dominates other cycles from 1974 to the present. Most importantly, it could see that the cycles of sunspot activity are evolving to low magnitudes, suggesting a decline, possibly into a grand minimum.

Fig. 8b illustrates the evolution in amplitude of geomagnetic activity. It shows that the HC increased from the beginning of the time-series to around 1880 and declined to low amplitudes thereafter reaching a minimum in 1940. It dominated over SB and the GB between 1868 and 1909. It rose again in magnitude until its peak was attained in 1997 before a final plunge. The GB, which has increased in magnitude from the beginning of the series, took dominance over the other cycles from 1908 to 2006, reaching its peak value in 1983 before a final plunge. The SB and HC were in the depending phase after about 1875, reaching some minimum values around the early 1940s. This observation appears to be consistent with the decrease in global surface temperature observed from 1944 (Fig. 3). Also, all the cycles reached their maximum amplitudes at different times. The GB reached its maximum level between 1960 and 1980. The HC reached its maximum level between 1980 and 2000. However, the leading cycles (GB and HC) declined rapidly after. It is observed that the SB increased in level after 1980 till the end of the series. Fig. 8c shows the plot of the trends and evolution in time of the magnitudes of the SB, HC and GB of annual mean global surface temperatures. It is found that the GB dominated the other two up to about 1922. The HC then took dominance over the others to the end of the time series. It is noted that the low-frequency HC and GB have continuously increased from the beginning of the series. The SB oscillated with very low amplitudes until after 1980 when it increased sharply. All the three cycles exhibit the tendency to decrease in level toward the end of the series.

4. Summary and Conclusions

In this study, the cyclic properties of sunspot activity, geomagnetic activity and global surface temperature were investigated using trend, spectral and wavelet analyses. These analyses clearly show that low frequency cycles of decadal to centennial timescales run in the background of the eleven-year cycle. The eleven-year running mean showed a trend of cyclicity of sunspot activity in the Gleisberg cycle range (between 99 to 114 years per cycle) and a bi-centennial cycle of approximately 227 years/cycle. Evidence of the bi-centennial cycle had been found in the natural archives as in Ref. [14] which identified a cycle length of 210 years. Spectral analysis revealed three peaks in all three series corresponding to eleven-year Schwabe cycle, the half-century cycle and Gleisberg cycle of slightly varying cycle lengths. The strongest cycle in sunspot and geomagnetic activity series is the Schwabe cycle. Schwabe and Gleisberg cycles are not significant compared to the half-century cycle in the global surface temperature series. It suggests that the half-century cycle of global surface temperature variability may be related to those of solar and geomagnetic activities.

Wavelet analysis reveals three peaks in solar and geomagnetic activities corresponding to the Schwabe, half-century and Gleisberg cycles respectively. However, it reveals only a peak corresponding to the half-century cycle in the global surface temperature series. It suggests a link between the solar and geomagnetic activities with global surface temperature series at a low-frequency cycles. The regression model suggests a recovery of solar activity from the Maunder Minimum and that the expected grand episode after the Modern Maximum will most likely be a minimum. The evolution of the amplitudes of the low-frequency cycles of solar and geomagnetic activities to lower values suggests a possible descent into a new grand episode which is expected to be a minimum. The evolution of the amplitudes of Schwabe, half-century and Gleisberg cycles of global surface temperature also indicate the tendency toward lower values. Thus, the low-frequency cycles of global surface temperature variability responses to the low-frequency components of solar and geomagnetic activity.

Conflict of interest statement
The authors declare that they have no conflict of interest in relation to this research, whether financial, personal, authorship or otherwise, that could affect the research and its results presented in this paper.
CRediT author statement
Efiong A. Ibanga: Conceptualization, Methodology, Writing- Original draft preparation; Etido P. Inyang: Software, Investigation, Data curation; Godwin A. Agbo: Visualization; Validation, Supervision.
The final manuscript was read and approved by all authors.

Acknowledgement

The authors express their gratitude to the organizations that generated the data used in this investigation.

References

1 Ibanga E.A., Agbo G. A., Inyang E. P., Ayedun F., Onuora L.O. (2020) Prediction of Solar Cycles: Implication for the Trend of Global Surface Temperature. *Communication in Physical Sciences*. 6(2), 882 – 890. Available at https://journalcps.com/index.php/volumes

2 Petrovay K. (2020) Solar cycle prediction. *Living Rev Sol Phys.* 17, 2-10. DOI:10.1007/s41116-020-0022-z(0123456789.

3 Kim J.H., Chang H.Y. (2014) Spectral Analysis of Geomagnetic Activity Indices and Solar Wind Parameters. *Journal of Astronomy and Space Science*. 31(2), 159 – 167. DOI: 10.5140/JASS.2014.31.2.159.

4 Okoh D.I., Seemala G.K., Rabiu A.B., Uwamahoro J., Habarulema J.B., Aggarwal M. (2018) Hybrid Regression-Neural Network (HR-NN) Method for Forecasting the Solar Activity. *Space Weather.* 16 (9), 1424-1436. DOI:10.1029/2018SW001907.

5 Hanslmeier A., Brajša R. (2010) The chaotic solar cycle I. Analysis of cosmogenic ^{14}C-data. *Astronomy and Astrophysics*. 509, A5. DOI:10.1051/0004-6361/200913095.

6 Peguero J.C., Carrasco V.M.S. (2023) A Critical Comment on "Can Solar Cycle 25 Be a New Dalton Minimum?" *Solar Physics*. 298: 48. DOI:10.1007/s11207-023-02140-7.

7 Kasde S.K; Sondhiya D.K., Gwal A.K. (2016) Analysis of Sunspot Time Series During the Ascending Phase of Solar Cycle 24 Using the Wavelet Transform. *American Journal of Modern Physics.* 5(5): 79 – 86. DOI:10.11648/j.ajmp.20160505.11.

8 Kristof P. (2020) Solar cycle prediction. *Living Reviews in Solar Physics*, 17: 2. DOI:10.1007/s41116-020-0022-z.

9 Muraki Y., Shibata S., Takamaru H., Oshima A. (2023) The 48-Year Data Analysis Collected by Ngoya Muon Telescope – A Detection of Possible (125±45)-Day Periodicity. *Universe.* 9, 372-387. DOI:10.3390/universe9090387.

10 Torrence C., Compo G.P. (1998) A Practical Guide to Wavelet Analysis. *Bulletin of the American Meteorological Society*. 79(1), 61–78. DOI:10.1175/1520-0477(1998)079<0061:APGTWA>2.0.CO;2.

11 Riabova S. (2018) Application of wavelet analysis to the analysis of geomagnetic field variations. *Journal of Physics: Conference Series*. 1141: 012146. DOI:10.1088/1742-6596/1141/1/012146.

12 Liu Y., San Liang X., Weisberg R.H. (2007) Rectification of the Bias in the Wavelet Power Spectrum. *Journal of Atmospheric and Oceanic Technology*. 24, 2093–2102. DOI:10.1175/2007JTECHO511.1.

13 Cazelles B., Chavez M., Berteaux D., Menard F., Vik J.O., Jenouvrier S., Stenseth N.C. (2008) Wavelet analysis of ecological time series. *Oecologia*. 156 (2): 287–304.

14 Mohamed A.E., Eman S., Aly A., Shady E.M. (2010) Spectral Analysis of Solar Variability and their Possible Role on the Global Warming. *Journal of Environmental Protection*. 1, 111-116.

AUTHORS' INFORMATION

Ibanga, Efiong A. - Dr. (Sci.), Professor, Department of Physics, National Open University of Nigeria, Jabi, Abuja-Nigeria Victoria Island, Lagos, Nigeria; ORCID iD 0000-0002-5452-0613; eibanga@noun.edu.ng

Inyang, Etido P. – Dr. (Sci.), Professor, Department of Physics, National Open University of Nigeria, Jabi, Abuja-Nigeria Victoria Island, Lagos, Nigeria; ORCID iD: 0000-0002-5031-3297; etidophysics@gmail.com

Agbo, Godwin A. Professor, Department of Industrial Physics, Ebonyi State University, Abakaliki, Nigeria; profgodwinagbo@gmail.com